Soil & Tillage Research 189 (2019) 15–24

Contents lists available at ScienceDirect

Soil & Tillage Research

journal homepage: www.elsevier.com/locate/still

# Impact of sample dimensions, soil-cylinder wall friction and elastic properties of soil on stress field and bulk density in uniaxial compression tests

Renato P. de Lima[a,*], Thomas Keller[b,c]

[a] Department of Agricultural Engineering, Federal Rural University of Pernambuco, Rua Dom Manoel de Medeiros, s/n, Dois Irmãos, 52171-900, Recife, PE, Brazil
[b] Swedish University of Agricultural Sciences, Department of Soil & Environment, Box 7014, SE-75007, Uppsala, Sweden
[c] Agroscope, Department of Agroecology & Environment, Reckenholzstrasse 191, CH-8046, Zürich, Switzerland

ARTICLE INFO

*Keywords:*
Compressive properties
Coefficient of friction
Confined soil compression test
Poisson's ratio
Finite element model

ABSTRACT

Compressive properties of arable and forest soils are typically derived from data obtained in uniaxial confined compression tests. However, the stress field, final state of compression and thus compressive properties derived from such tests are dependent on sample dimensions, soil-cylinder wall friction and soil material properties. In this study, we analysed the stress field and bulk density distribution within a cylindrical soil sample under uniaxial compression, and how these are affected by sample dimension, soil-cylinder wall friction and elastic properties of soil. For this, we modelled a uniaxial compression test using the finite element method (FEM) and performed simulations for a range of sample diameter to height ratios ($D/h$), different values of soil-wall friction coefficient ($\mu$) and different soil elastic properties (Young's modulus and Poisson's ratio). We use experimental data to validate the findings. The results showed a high impact of soil-cylinder wall friction on the stress field within the sample. This resulted in stress concentration at the top of sample edges (walls) and decreasing stresses at the bottom of the sample. However, the relative impact of soil-wall friction on sample average behaviour decreased with increasing $D/h$. These results suggest that the effect of soil-wall friction on sample-average bulk density cannot be neglected unless $D/h > 8$. Correction of bulk density for $\mu$ and $D/h$ could be a practical way to compare data obtained in laboratories using different sample sizes.

## 1. Introduction

Soil compaction due to agricultural or forest traffic adversely impacts several soil functions, including water and nutrient cycling, agricultural and forestry production and habitat for soil organisms. Prediction of compaction risks prior to field traffic, e.g. using decision support tools (Horn and Fleige, 2009; Stettler et al., 2014), can help avoid soil compaction. Prediction of compaction risks requires knowledge of soil mechanics, in particular soil compressive properties (recompression or swelling index, compression index, precompression stress).

Compressive properties of arable and forest soils are typically determined from data obtained in uniaxial confined compression tests. Although triaxial tests could more realistically mimic stress conditions in the field, uniaxial tests are used because they are simpler and cheaper, and therefore available in many laboratories and accessible for many researchers. Moreover, a uniaxial stress state is thought to represent the stress-strain state of the subsoil under wheeling (Koolen, 1974). Prevention of compaction in the subsoil is of critical importance because of the low recovery potential of subsoil (van den Akker et al., 2003; Schjønning et al., 2015).

A limitation of the uniaxial compression test is that mean normal stress, $\sigma_m$, is not measured. Volumetric deformation (e.g. increase in bulk density, decrease in void ratio) is often related to the (logarithm of) vertical normal stress, $\sigma_v$, but in fact volumetric deformation is not related to $\sigma_v$ but to $\sigma_m$ (e.g. Davis and Selvadurai, 1996). For a cylindrical stress state, as in a cylindrical sample under uniaxial compression, $\sigma_m = ⅓ [\sigma_v + 2\sigma_r]$, where $\sigma_r$ is the radial stress. The ratio of $\sigma_r$ to $\sigma_v$ is known as the coefficient of earth pressure. For zero lateral strain, as is the case under confined conditions, $K_0 = \sigma_r/\sigma_v$, where $K_0$ is the "at-rest coefficient of earth pressure". Hence, knowledge of $K_0$ would allow $\sigma_m$ to be computed. For uniaxial confined compression tests, Koolen and Kuipers (1983) suggest a value for $K_0$ of 0.5.

However, it has been reported that the stress field within a sample is

* Corresponding author.
*E-mail addresses:* renato_agro_@hotmail.com, renato.lima@bag.ifmt.edu.br (R.P. de Lima).

https://doi.org/10.1016/j.still.2018.12.021
Received 22 June 2018; Received in revised form 17 October 2018; Accepted 21 December 2018

affected by friction at the soil-cylinder wall interface (Koolen, 1974; Rosine and Sabbagh, 2015). For example, Koolen (1974) found that $\sigma_v$ at the top and bottom of a sample are distinctly different and vary as a function of sample size and friction between soil and cylinder wall. Hence, the ratio of $\sigma_r$ to $\sigma_v$, i.e. $K_0$, and therefore estimates of $\sigma_m$, should also be a function of soil-wall friction. It has been shown that the influence of soil-wall friction on the overall behaviour of a sample can be reduced by increasing the ratio of sample diameter, $D$, to sample height, $h$ (Koolen, 1974; Rosine and Sabbagh, 2015). Therefore, to minimise the influence of soil-wall friction, a minimum $D/h$ is recommended for uniaxial compression tests (Koolen, 1974; American Standard D4318, 2010; British Standard BS1377, 1990). The recommended $D/h$ is within the range 2.5 (American Standard D4318, 2010) to 4 (British Standard BS1377, 1990). However, the influence of soil-wall friction is not zero at these $D/h$ values. Koolen (1974) showed that while friction effects are small for $D/h > 2.5$, they influence soil behaviour even at larger $D/h$.

It is well known that soil-wall friction affects soil deformation and hence the change in bulk density (or void ratio) during confined uniaxial compression (Kolay and Bhattacharya, 2008), and therefore also the magnitude of compressive properties derived from confined compression test data (Rosine and Sabbagh, 2015). However, quantitative knowledge of the effect of soil-wall friction and its interaction with sample dimensions on the stress field within a sample and the bulk density under uniaxial confined compression remains limited. Analyses of compression data usually do not consider friction effects. Moreover, different laboratories typically use different sample sizes (including samples with $D/h$ ratios that are smaller than recommended to minimise friction effects). Without knowledge of the impact of soil-wall friction as a function of $D/h$ on soil behaviour during compression, comparisons of compressive properties derived from samples with different sizes are not possible. This hampers e.g. development of pedotransfer functions for soil compressive properties. As stated by Koolen (1974), the determination of compressive properties of soil should not be influenced by sample size or the test device used.

The objectives of this study were to analyse the stress field and bulk density distribution within a cylindrical soil sample under uniaxial compression, and determine how these are affected by sample dimension, soil-cylinder wall friction and elastic properties of soil. For this, we modelled a uniaxial compression test using the finite element method and performed simulations for a range of sample diameter to height ratios, for different soil-wall friction coefficients and for different soil elastic properties. We complemented the simulations with experimental data in order to validate the findings.

## 2. Material and methods

### 2.1. Finite element model

Simulations were carried out using finite element modelling (FEM) within the framework of COMSOL Multiphysics Version 5.2, to investigate the influence of sample dimensions, friction between soil and cylinder wall and elastic properties of the soil on stress field and bulk density in soil cores in confined compression tests. We reproduced a confined compression test by applying a surface pressure, $p_0$, of 200 kPa acting on a steel plate (0.003 m thick, diameter equal to that of the soil core) on soil confined in an aluminium cylinder ring (wall width 0.003 m). The properties of the plate and the cylinder ring were taken from the material library available in COMSOL Multiphysics and are given in Table 1.

The model was formulated as an axisymmetric problem, with the dimensions described in Fig. 1. The geometry consisted of an assembly of three solid objects (plate, cylinder and soil) and was meshed with 4500 elements. The displacements in the radial (horizontal) direction, $u$, and in the axial (vertical) direction at the lower boundary, $w$, were restricted (i.e. equal to 0). Mesh and boundary conditions of the finite element model are given in Fig. 1A.

**Table 1**
Elastic properties of the plate and cylinder ring used for finite element simulations, which reflect the properties of steel and aluminium, respectively.

| Elastic properties | Plate (steel) | Cylinder (aluminium) |
|---|---|---|
| Bulk density (Mg $m^{-3}$) | 7.85 | 2.70 |
| Young's modulus (kPa) | 205,000,000 | 70,000,000 |
| Poisson's ratio (-) | 0.28 | 0.33 |

We used a linear-elastic model as a constitutive relationship based on Hooke's law. For an elastic material, the incremental stress tensor, $d\sigma_{ij}$, is related to the incremental strain tensor, $d\varepsilon_{ij}$, by (e.g., Keller et al., 2016):

$$d\sigma_{ij} = D_{ij} d\varepsilon_{ij} \quad (1)$$

where $D_{ij}$ is an elastic constitutive matrix, formed by independent equations relating stresses and strains. The incremental elastic strain can be expressed following Hookean elastic behaviour:

$$d\varepsilon_{ij} = \frac{1+\nu}{E} d\sigma_{ij} - \frac{\nu}{E} d\sigma_{kk}\delta_{ij} \quad (2)$$

where $\nu$ is Poisson's ratio, $E$ is Young's modulus (also termed the modulus of elasticity), $d\sigma_{kk}$ is the incremental volumetric stress tensor and $\delta_{ij}$ is the Kronecker delta. Therefore, the magnitude of the deformation is dependent on the stress ($\sigma$) and material properties ($E$,$\nu$).

Contact pairs were created between soil and cylinder wall and between soil and plate (Fig. 1B). The contact defines boundaries where two different parts (materials) can come into contact but cannot penetrate each other under deformation, and this can be modelled with or without friction. Since only vertical stress was applied at the top of the sample, in this study the contact between plate and soil (Fig. 1B) was assumed to be frictionless. For the contact between soil and cylinder wall, the simulations were performed with and without friction (see below). Musson and Carlson, (2014) report two main methods for modelling contact, both of which are available in COMSOL Multiphysics: the Lagrangian method and the penalty method. The Lagrangian method is considered the classical approach, but it can lead to long computation times or convergence problems (Musson and Carlson, 2014), as we experienced during initial simulations. The penalty method is simple and less sensitive to numerical convergence. In this study, we used the penalty method to model the contact, which can be described by (e.g.Musson and Carlson, 2014):

$$T_{np} = \begin{cases} T_n - p_n g & \text{if } g \le 0 \\ T_n \exp(-\frac{p_n g}{T_0}) & \text{otherwise} \end{cases} \quad (3)$$

where $T_{np}$ represents the penalised contact pressure, $T_n$ is the estimated contact pressure, (assumed here as the applied pressure, $p_0$), $g$ is the gap distance and $p_n$ is the contact normal penalty factor, which is defined as:

$$p_n = \xi \frac{E}{h_{min}} \quad (4)$$

where $\xi$ is the user-defined penalty factor, *hmin* is the minimum mesh element size and $E$ is the elastic modulus. Friction between soil and cylinder wall was computed using the classic Coulomb friction model, which can be expressed as:

$$F_{force} = \mu F_n \quad (5)$$

where $F_{force}$ is the friction force, $\mu$ is the coefficient of friction and $F_n$ is the normal force.

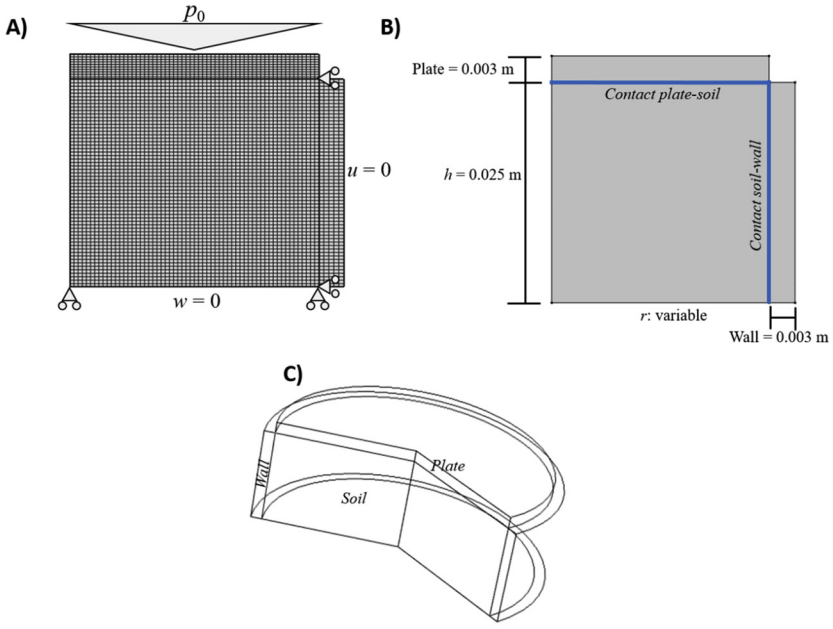


**Fig. 1.** A) Mesh, applied surface pressure (acting on the plate) $p_0$, and boundary conditions of the finite element model, where $u$ is the displacement in the radial (horizontal) direction and $w$ is the displacement in the axial (vertical) direction at the bottom of the sample. B) Dimensions and contacts assumed for the sample, plate and cylinder, where the radius ($r$) is variable (different ratios of diameter to height ($h$) were considered for the simulations, see text for details). C) 3-D model illustration.

### 2.2. Coefficient of soil-cylinder wall friction, sample dimensions and soil properties

In a first set of simulations, we analysed the effects of the coefficient of soil-wall friction ($\mu$) and sample dimensions. We set sample height ($h$) at 0.025 m (Fig. 1B) and varied the sample diameter ($D$) from 0.0188 to 0.025, 0.05, 0.075, 0.125 and 0.20 m, corresponding to a sample diameter to height ($D/h$) ratio of 0.75, 1, 2, 3, 5 and 8, respectively. We also assumed contact between soil and cylinder wall when the soil is compressed (Fig. 1B), and tested $\mu$ values of 0, 0.1, 0.2, 0.3, 0.4, 0.5, 0.6, 0.7 and 0.8. All these scenarios were simulated considering the elastic properties of the plate and cylinder described in Table 1 and soil properties based on experimental data reported in Keller et al. (2016), with bulk density 1.30 Mg m$^{-3}$, Young's modulus (kPa) 3,000 kPa and Poisson's ratio 0.38.

In a second set of simulations, we analysed the effect of the elastic properties, i.e. Young's modulus and Poisson's ratio. We considered scenarios where Young's modulus of soil (elasticity modulus) was 2,000, 3,000, 4,000, 5,000 and 6,000 kPa, while keeping the bulk density and Poisson's ratio constant, and scenarios where Poisson's ratio (lateral deformation) was 0.25, 0.30, 0.35, 0.40, 0.45, while keeping Young's modulus and bulk density constant. The simulations were performed with the conditions of plate and cylinder elastic properties established in Table 1, under $\mu$ of 0 and 0.4 (i.e. with and without friction). The complete scenarios used in the second set of simulations are given in Table 2.

### 2.3. Experimental data: uniaxial compression tests with different sample dimensions

To compare simulation results with real data, we used data obtained in uniaxial confined compression tests carried out on undisturbed cylindrical soil samples with diameter 0.072 m and height 0.025, 0.05 or 0.1 m, resulting in values for $D/h$ of 2.88, 1.44 and 0.72, respectively. The samples were taken from a clay soil (62% clay, 20% silt, 18% sand, 0.8% organic matter content) in Uppsala, Sweden (59.9 °N, 17.6 °E). In order to obtain some variation in the experimental data, we sampled at 0.3 and 0.5 m depth, which differed in terms of bulk density. Five samples of each sample size were collected at each depth. In the laboratory, the samples were subjected to uniaxial compression using sequential loading with a loading time of 30 min per load and the following vertical stresses: 10, 25, 50, 75, 100, 200, 300, 400, 600 and 800 kPa. The samples were compressed at field water content, which was 0.29 and 0.34 kg kg$^{-1}$ at 0.3 and 0.5 m depth, respectively. Upon completion of the compression test, the samples were oven-dried (105 °C) and the bulk density was calculated from the measured strain at each load step. The compression index was obtained from linear regression through the virgin compression line.

## 3. Results

### 3.1. Impact of sample dimensions and soil-wall friction on stress field and final bulk density

The influence of $D/h$ ratio and the impact of soil-wall friction on the distribution of vertical stress ($\sigma_v$), radial stress ($\sigma_r$), the ratio of radial to vertical stress ($\sigma_r/\sigma_v$) and the final bulk density after compression ($BD_{final}$) within the soil sample are shown in Fig. 2. Without soil-wall friction (a frequent assumption, as mentioned elsewhere), i.e. for $\mu = 0$, the stresses and consequently $BD_{final}$ after compression were uniform within the whole sample, independent of sample dimensions. As Fig. 2 demonstrates, soil-wall friction (which occurs in reality but is often neglected) modified the stress pattern within the sample and the ratio of radial to vertical stress ($\sigma_r/\sigma_v$), and this also affected the $BD_{final}$ distribution. The coefficient of soil-wall friction of 0.4 used in Fig. 2 represents a typical value (Koolen, 1974). Soil-wall friction caused

**Table 2**
Elastic properties of the soil used in the finite element simulations to evaluate effects of Young's modulus and Poisson's ratio.

| Soil property | 1: varying Young's modulus | 2: varying Poisson's ratio |
|---|---|---|
| Bulk density (Mg m$^{-3}$) | 1.30 | 1.30 |
| Young's modulus (kPa) | 2,000, 3000, 4,000, 5000 or 6000 | 3000 |
| Poisson's ratio (-) | 0.38 | 0.25, 0.30, 0.35, 0.40 or, 0.45 |

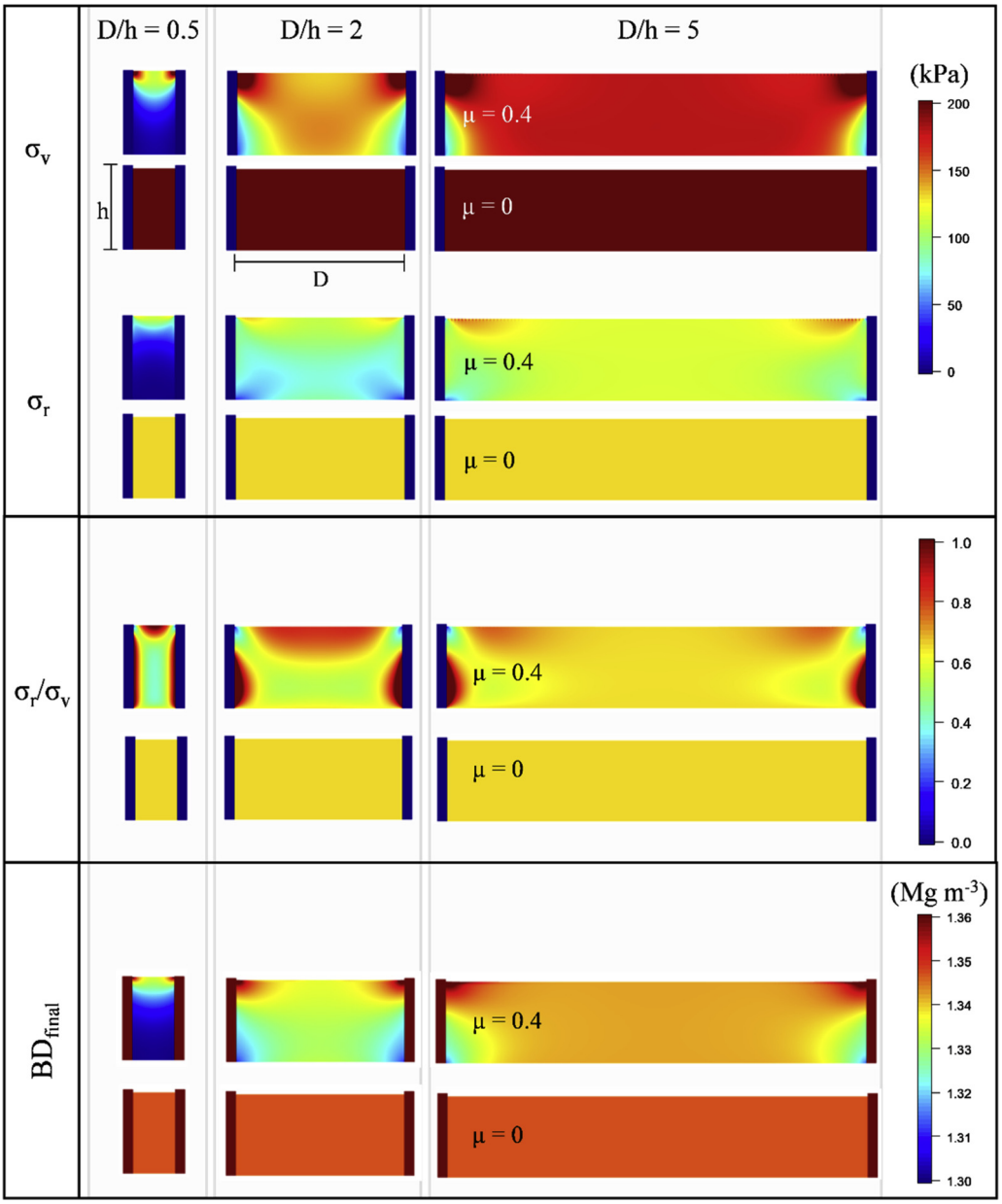


**Fig. 2.** Influence of sample diameter ($D$) to height ($h$) ratio (left: $D$/h = 0.5; centre: $D/h$ = 2; left: $D/h$ = 5) and coefficient of friction ($\mu$) (top graphs: $\mu$ = 0.4; bottom graphs: $\mu$ = 0) on the distribution of vertical stress ($\sigma_v$), radial stress ($\sigma_r$), the ratio of radial to vertical stress, $\sigma_r/\sigma_v$, and final bulk density ($BD_{final}$) after compression. Simulations were made for an applied surface pressure ($p_0$) of 200 kPa and an initial $BD$ of 1.3 Mg m$^{-3}$, with material properties as given in Table 1.

stress concentration at the top of the sample edges (walls), but decreased stresses at the bottom of the sample edges (Fig. 2). This resulted in a higher $BD_{final}$ at the upper sample edges and a lower $BD_{final}$ along the walls at the bottom of the sample.

Soil-wall friction effects on the pattern of stress field and $BD_{final}$ close to the walls were similar for all $D/h$, but the overall effect (e.g. on the sample-average $BD_{final}$) was dependent on $D/h$ (Fig. 2). For example, the stress at the bottom of the sample was close to the applied surface pressure ($p_0$ = 200 kPa) for $D/h$ = 5, but less than 50 kPa for $D/h$ = 0.75 (Fig. 2). Consequently, $BD_{final}$ was similar to $BD_{initial}$ at the bottom of the sample for $D/h$ = 0.75. Soil-wall friction also affected $\sigma_r/\sigma_v$, which increased at the walls due to soil-wall friction.

The ratio of vertical stress, $\sigma_v$, at the centre of the sample to the applied surface pressure, $p_0$, is shown in Fig. 3 for different $D/h$ and as a function of $\mu$. The ratio of $\sigma_v$ to $p_0$ equals 1.0 for $\mu$ = 0, for any sample dimension (Fig. 3). With increasing soil-wall friction, $\sigma_v/p_0$ decreased and the smaller $D/h$, the stronger the decrease (Fig. 2). Thus the $\sigma_v/p_0$ was only around 0.4 at the top and 0.2 at the bottom of the sample for $D/h$ = 0.75, while $\sigma_v/p_0$ at the centre of the sample was not affected by $\mu$ for $D/h$ = 8 (Fig. 3).

The ratio of $\sigma_r$ to $\sigma_v$ at the sample centre is shown in Fig. 4. For $\mu > 0$, $\sigma_r/\sigma_v$ was close to 1 at the top of the sample, decreased in the middle of the sample and increased again at the bottom. This general pattern was found for any $D/h$, but the impact of $\mu$ on $\sigma_r/\sigma_v$ at the centre of the sample decreased with increasing $D/h$ to no effect for $D/h > 3$.

Bulk density is a function of $\sigma_{mean}$, and hence was also affected by $\mu$ and $D/h$. For $\mu$ = 0, $BD_{final}$ was 1.35 Mg m$^{-3}$ at any depth and unaffected by sample dimensions (Fig. 5). $BD_{final}$ at the sample centre decreased with decreasing $D/h$ and with increasing $\mu$. $BD_{final}$ at the sample centre was uniform with depth for $D/h > 3$, but was affected (i.e. reduced) by $\mu$ even at $D/h > 3$. The sample-average final bulk density $BD_{final,Mean}$ for different $D/h$ and as a function of $\mu$ is given in Fig. 6. As mentioned above, $BD_{final,Mean}$ was 1.35 Mg m$^{-3}$ for $\mu$ = 0 (Fig. 6A). As Fig. 6 shows, $BD_{final,Mean}$ was only marginally affected by $\mu$

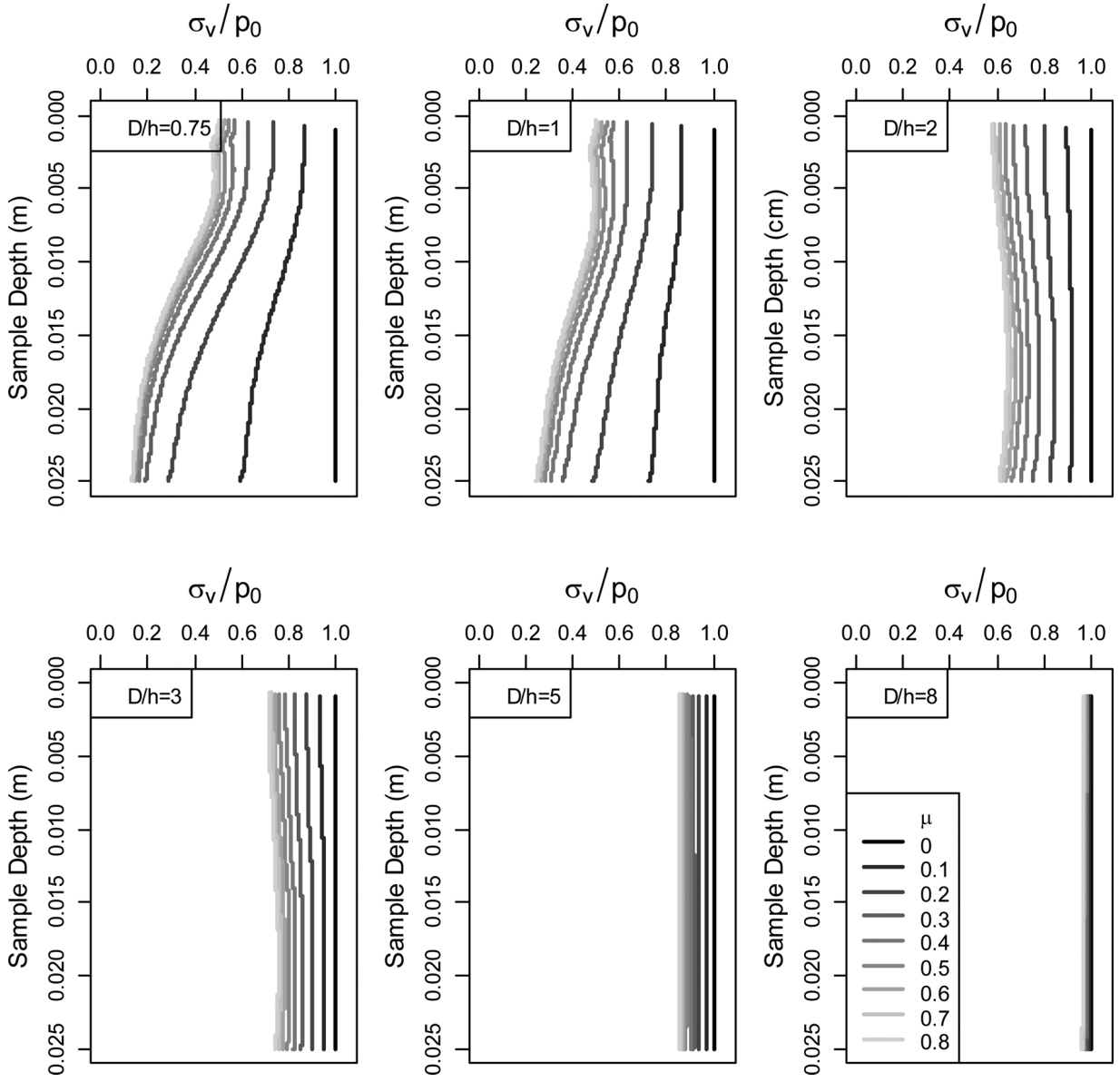


**Fig. 3.** Ratio of vertical stress at the centre of the sample ($\sigma_v$) to applied surface stress ($p_0$) as a function of sample depth for different sample diameter to height ($D/h$) ratios and different values of coefficient of soil-wall friction ($\mu$).

for $D/h = 8$, whereas it was $< 1.35$ Mg m$^{-3}$ for $D/h < 8$ and $\mu > 0$. The smaller $D/h$, the larger the impact of $\mu$ on $BD_{final,Mean}$ (Fig. 6B). The effect of $\mu$ on $BD_{final,Mean}$ increased up to around $\mu = 0.4$, and was little further affected for $\mu > 0.4$ (Fig. 6). The impact of $D/h$ on bulk density is demonstrated in Fig. 7A, which shows data obtained in uniaxial confined compression tests on undisturbed soil samples taken from a Swedish clay soil. The samples had diameter 7.2 cm and height either 2.5, 5 or 10 cm, resulting in $D/h$ of 0.72, 1.44 and 2.88, respectively. The increase from initial to final bulk density at an applied stress of 200 kPa increased with increasing $D/h$, e.g. the bulk density increased by only ~0.05 Mg m$^{-3}$ for $D/h = 0.72$, whereas the increase was almost 0.15 Mg m$^{-3}$ for $D/h = 2.88$. These differences had a significant impact on the magnitude of compressive properties derived from uniaxial compression data. As Fig. 7B illustrates, the compression index decreased with decreasing $D/h$, caused by the lower bulk density for lower $D/h$, which in turn was due to the increasing overall impact of soil-wall friction with decreasing $D/h$.

### 3.2. Impact of soil mechanical properties on stress field and bulk density

Young's modulus had no impact on either $\sigma_v/p_0$ (Fig. 8A) or $\sigma_r/\sigma_v$ (Fig. 8B). Poisson's ratio ($\nu$) did not affect $\sigma_v/p_0$ when no soil-wall friction was assumed. However, $\sigma_v/p_0$ decreased with decreasing $\nu$ for $\mu > 0$ (Fig. 9A) and $\sigma_r/\sigma_v$ also decreased with decreasing $\nu$ (Fig. 9B). Therefore, $\nu$ also affected $\sigma_{mean}$, which not only influences bulk density but also compressive properties derived from uniaxial compression test data. The effect of different ratios of $\sigma_r$ to $\sigma_v$ (expressed as $K_0 = \sigma_r/\sigma_v$) on the location of the recompression line and the virgin compression lines and on the magnitude of the precompression stress are illustrated in Fig. 7C.

As expected, $BD_{final}$ was affected by Young's modulus (Fig. 8C) and Poisson ratio (Fig. 9C). $BD_{final}$ increased with decreasing $E$ and with decreasing $\nu$, i.e. the softer and more compressible the soil, the larger $BD_{final}$.

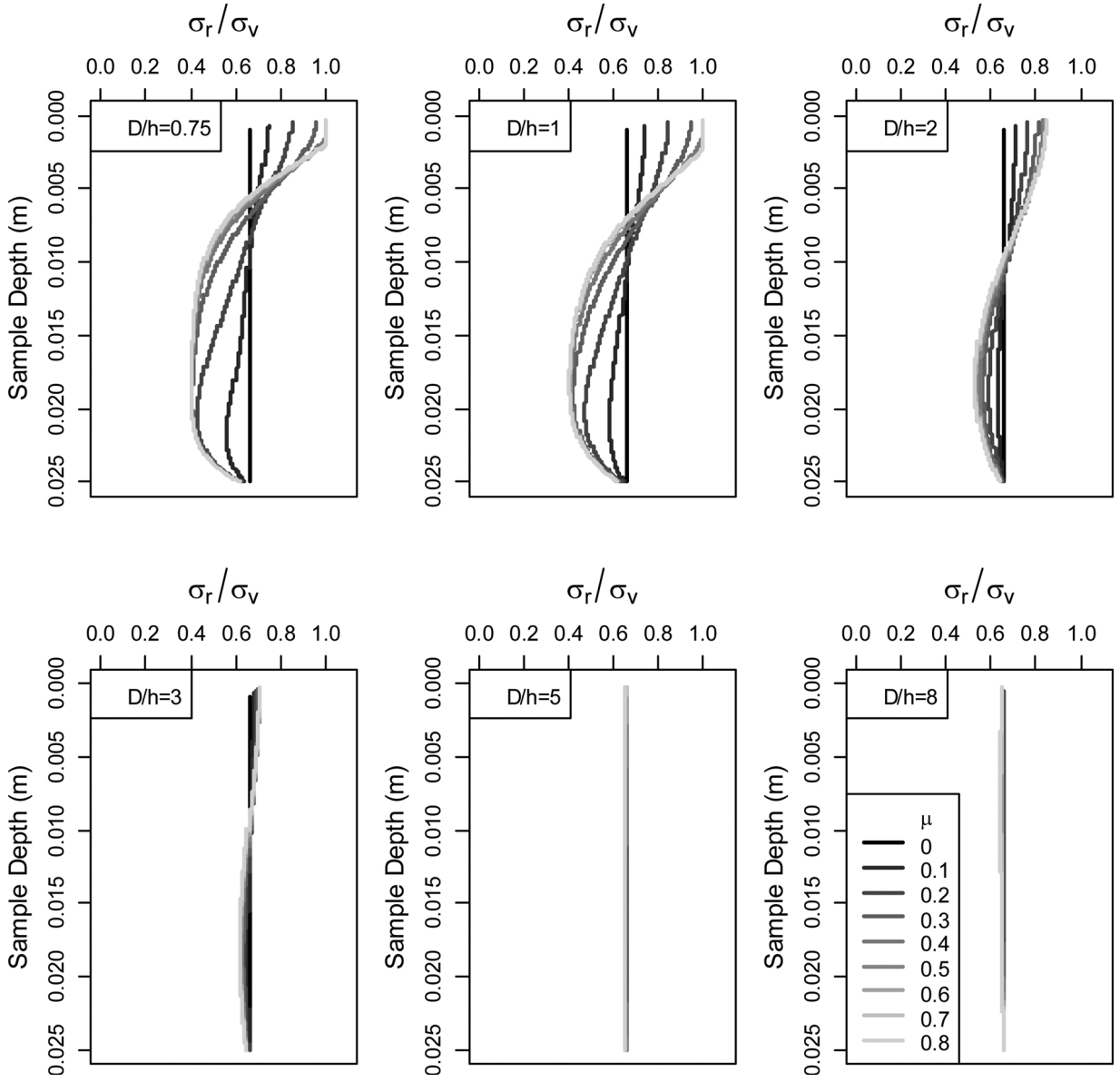


**Fig. 4.** Ratio of radial stress ($\sigma_r$) to vertical stress ($\sigma_v$) at the centre of the sample as a function of sample depth for different sample diameter to height ($D/h$) ratios and different values of coefficient of soil-wall friction ($\mu$).

## 4. Discussion

### 4.1. Stress distribution within the sample and the ratio of vertical stress to applied stress

Analysis of uniaxial compression data and determination of compressive properties from these data typically assume that the stress within the sample is uniform and that it is the same as the applied stress. We show that this only holds true for $\mu = 0$, for which $\sigma_v = p_0$ at any location within the sample, independent of $D/h$ (Figs. 2 and 3). Similarly, Taylor (1942) concluded that the inter-granular vertical stress acting within the sample ($\sigma_v$) will only equal the applied stress on top of the sample ($p_0$) if there is no friction at the soil-cylinder wall interface.

The stress field within the sample was significantly affected by soil-cylinder wall friction (Figs. 2 and 3). The coefficient of friction between soil and metal depends on soil texture, water content and metal properties and roughness (Tsubakihara et al., 1993). A typical value for $\mu$ is 0.4, but values between 0.3 and 0.6 have been used (e.g. Koolen, 1974; McKenzie et al., 2013; Naderi-Boldaji et al., 2018). Soil-cylinder wall friction imposes resistance to the relative motion of the soil against the solid aluminium face (Rosine and Sabbagh, 2015), thus decreasing soil compression. As a consequence, stress decreases with depth along the cylinder walls (Fig. 2). While the impact of $\mu$ seems marginal for large $D/h$, it is significant and may reach the centre of the sample for small $D/h$. For example, $\sigma_v$ at the bottom of the sample was close to zero for $D/h = 0.5$ and $\mu = 0.4$ (Fig. 2). In contrast, for large $D/h$ (e.g. $D/h = 5$ in Fig. 2), $\mu$ only affected the areas close to the walls, while the stress at the centre of the sample was not affected. The role of $D/h$ on the overall impact of $\mu$ was also shown by e.g. Koolen (1974) and Rosine and Sabbagh (2015), and has resulted in a general recommendation for sample dimensions of $D/h > 2.5$ (American Standard D4318, 2010), $> 3$ (Koolen, 1974) and $> 4$ (British Standard BS1377, 1990).

### 4.2. Ratio of radial to vertical stress

The ratio of radial to vertical stress is an important quantity. Many studies apply uniaxial compression tests to obtain the compressive

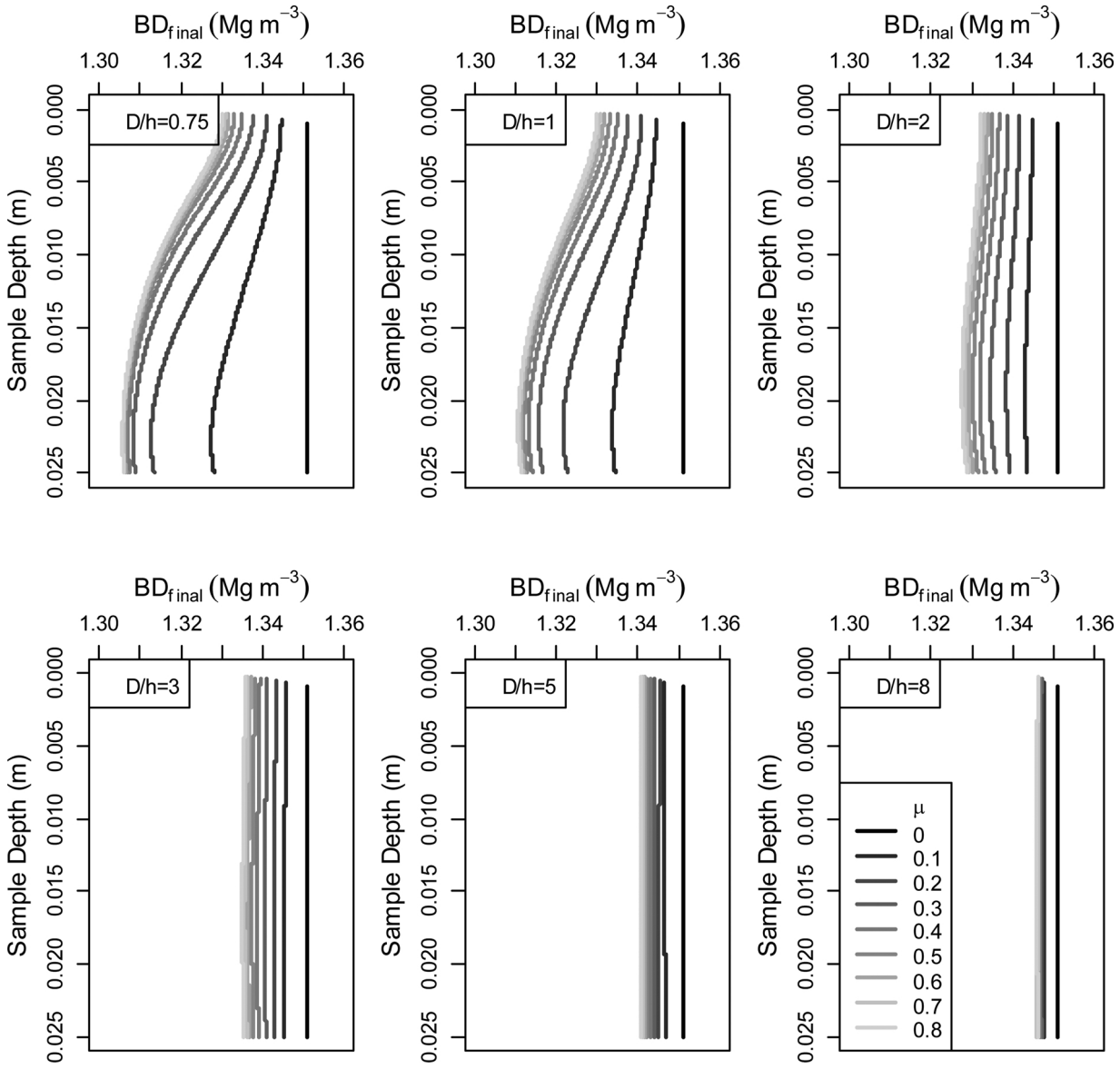


**Fig. 5.** Final bulk density after compression ($BD_{final}$) at the centre of the sample as a function of sample depth for different sample diameter to height ($D/h$) ratios and different values of coefficient of soil-wall frictions ($\mu$). The applied surface pressure ($p_0$) was 200 kPa, the initial bulk density was 1.3 Mg m$^{-3}$ and material properties are given in Table 1.

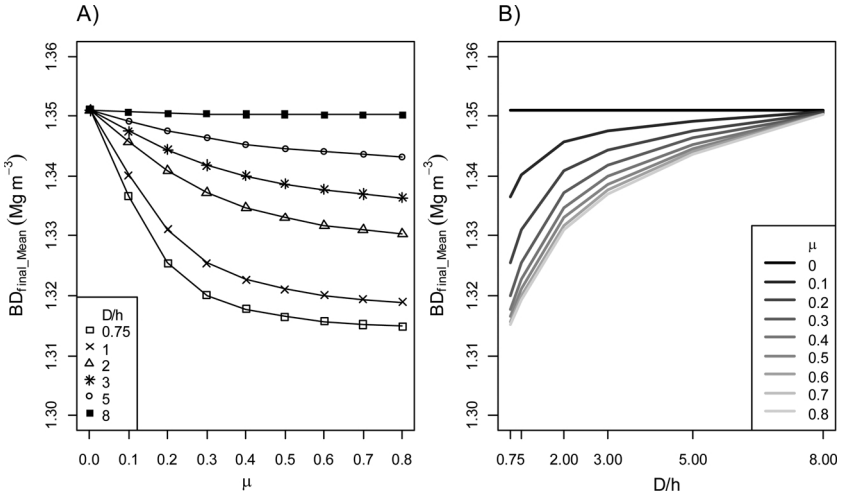


**Fig. 6.** A) Final (i.e. after compression) average bulk density of the whole sample ($BD_{final,Mean}$) as a function of coefficient of soil-wall friction ($\mu$) for different sample diameter to height ratios ($D/h$). B) Final bulk density ($BD_{final,Mean}$) as a function of $D/h$. The applied surface pressure ($p_0$) was 200 kPa, the initial bulk density was 1.3 Mg m$^{-3}$ and material properties are given in Table 1.

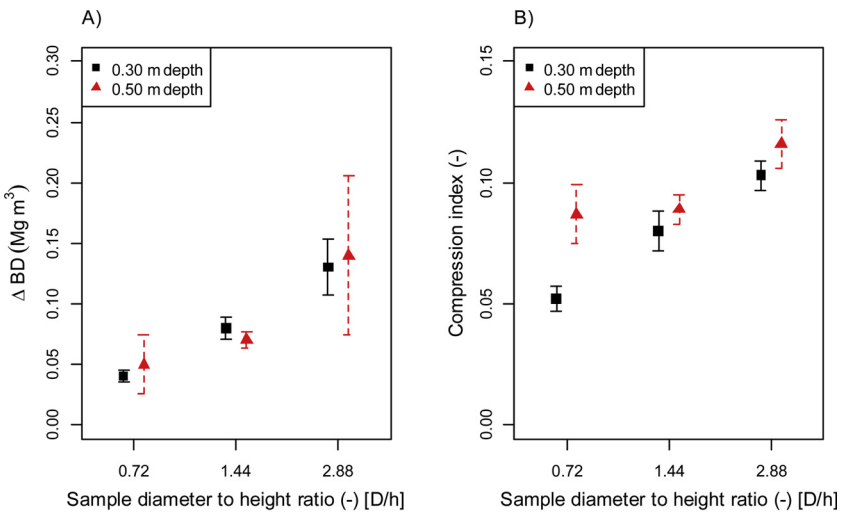


**Fig. 7.** A) Measured bulk density increase $\Delta BD$ due to compression with 200 kPa surface pressure ($p_0$) for different ratios of sample diameter ($D$) to height ($h$) ($D/h$ = 0.72, 1.44 and 2.88, respectively). B) Compression index as a function of $D/h$. C) Compression curves, recompression line (RCL), virgin compression line (VCL) and precompression stress (large symbol) obtained by assuming $K_0$ = 0.25 (black symbols and lines) and $K_0$ = 0.82 (red symbols and lines). Data were obtained from uniaxial confined compression tests on undisturbed soil samples collected in a Swedish clay soil at two depths (0.30 and 0.50 m). (For interpretation of the references to colour in this figure legend, the reader is referred to the web version of this article).

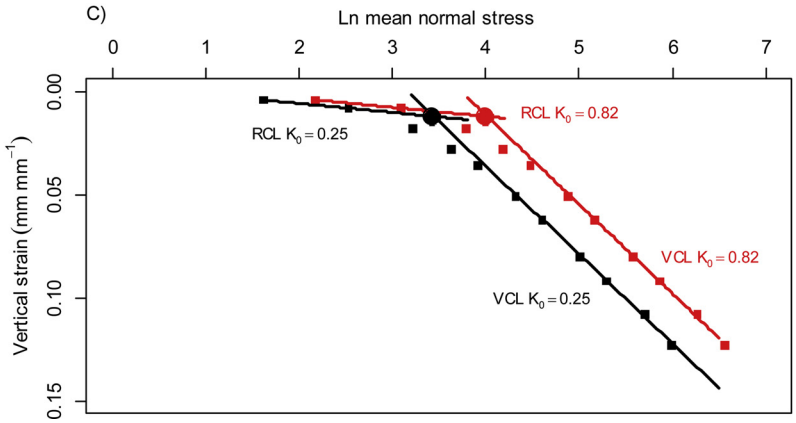


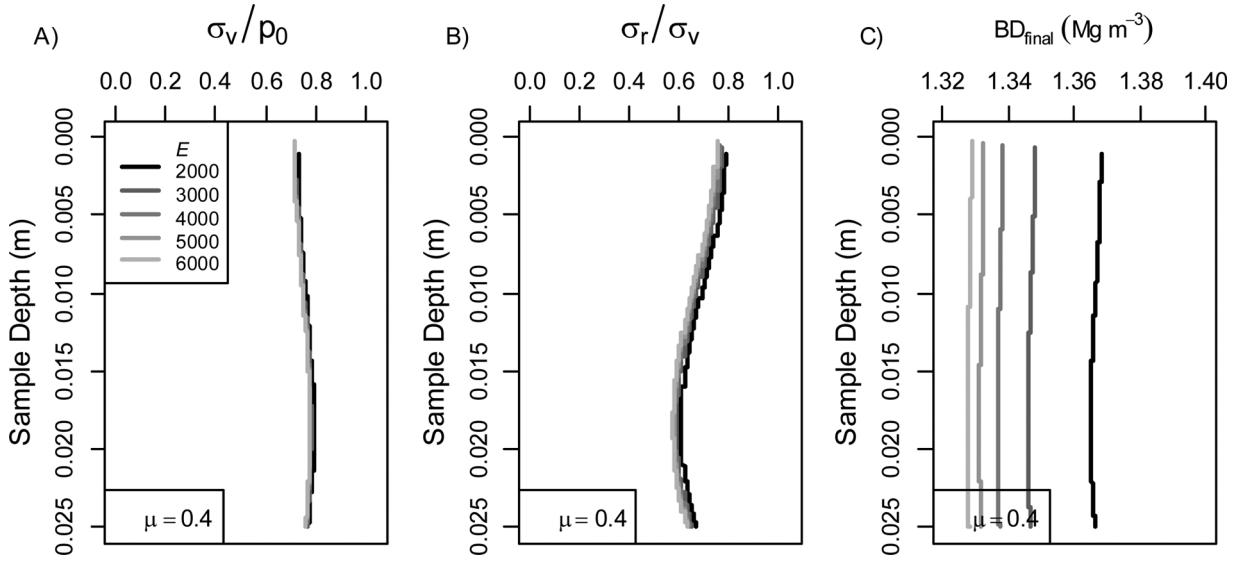


**Fig. 8.** A) Ratio of vertical stress at the centre of the sample ($\sigma_v$) to the applied vertical stress ($p_0$); B) ratio of radial stress at the centre of the sample ($\sigma_r$) to $\sigma_v$; and C) final (i.e. compression) bulk density ($BD_{final}$) at the centre of the sample for different values of Young's modulus ($E$) and coefficient of soil-cylinder wall friction, $\mu$, = 0.4. The initial (i.e. before compression) $BD$ was 1.30 Mg m$^{-3}$ (Table 2), sample diameter ($D$) was 0.06 m and sample height ($h$) 0.025 m, corresponding to $D/h$ = 2.4.

properties of soil, because uniaxial compression (oedometer) tests are simpler to perform than triaxial tests. However, compression (i.e. volume change) is a function of mean normal stress (e.g. O'Sullivan and Robertson, 1996), not vertical stress, although compressive properties are often determined from the relationship volume change (e.g. void ratio, bulk density) and the (logarithm) of vertical stress.

For a linear elastic problem in the case where there is no soil-wall friction, $K_0$ is a function of $\nu$ and given as $K_0 = (\nu/1\text{-}\nu)$ (e.g. Kirby,

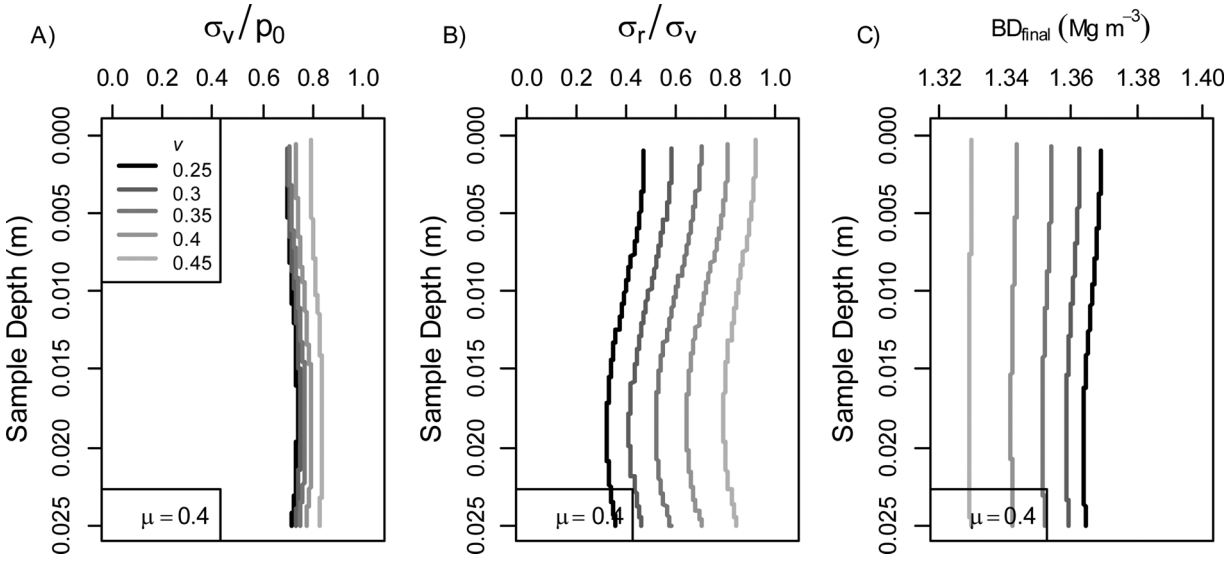


**Fig. 9.** A) Ratio of vertical stress at the centre of the sample ($\sigma_v$) to the applied vertical stress ($p_0$); B) ratio of radial stress at the centre of the sample ($\sigma_r$) to $\sigma_v$; and C) final (i.e. compression) bulk density ($BD_{final}$) at the centre of the sample for different values of Poisson's ratio ($\nu$) and coefficient of soil-cylinder wall friction, $\mu$, = 0.4. The initial (i.e. before compression) $BD$ was 1.3 Mg m$^{-3}$ (Table 2), sample diameter ($D$) was 0.06 m and sample height ($h$) 0.025 m, corresponding to $D/h$ = 2.4.

1999). In many studies, $K_0$ = 0.5 is assumed (e.g. Koolen, 1974; Keller et al., 2007; Lima et al., 2018). However, this only holds true for Poisson's ratio ($\nu$) = 0.33. This can be considered a typical value for soil (e.g. Défossez et al., 2003; Keller et al., 2016), but $\nu$ is a function of soil constituents (particle size distribution, organic carbon content) and soil conditions (bulk density, soil moisture). For example, Naderi-Boldaji et al. (2014) obtained a value of $\nu$ = 0.44 for a clay loam soil. For $\nu$ = 0.38 as assumed in our simulations (Table 1), $K_0 = \sigma_r/\sigma_v$ = 0.61 (*cf.* Fig. 4 for $\mu$ = 0). For incompressible material ($\nu$ = 0.5), $K_0$ = 1. Considering that $\nu$ for soils may be within the range 0.2-0.45 (e.g. Kirby, 1999; Défossez et al., 2003), $K_0$ may vary between 0.25 and 0.82. The illustrative example in Fig. 7C shows how this affects the ln $\sigma_{mean}$-strain curve and the location of the recompression and virgin compression lines. Different values for $K_0$ do not affect the magnitude of the recompression or compression index (i.e. slope of the recompression and virgin compression line, respectively), which can easily be shown by applying the logarithm rules. However, because the intercepts (and hence the location) of the recompression and virgin compression lines differ for different values of $K_0$, the magnitude of the precompression stress is also affected by $K_0$ (Fig. 7C). In our example, the precompression stress varied between 31 ($K_0$ = 0.25) and 55 kPa ($K_0$ = 0.82). Unfortunately, $\nu$ is seldom measured, but as shown here is an important soil property that should be measured when determining soil compressive properties. It can conveniently be obtained from uniaxial compression tests by combining confined and unconfined tests (Eggers et al., 2006), using separate samples for practical reasons (Naderi-Boldaji et al., 2014).

As discussed in Section 4.1, friction between soil and cylinder wall affected the stress field within the sample, and hence also $\sigma_r/\sigma_v$ (Figs. 2 and 3). The impact of soil-cylinder wall friction on $\sigma_r/\sigma_v$, and hence $K_0$, is not easy to compute, since this involves heterogeneous distribution of stress within the sample (Fig. 2), and since $\sigma_r/\sigma_v$ changes from the centre to the edge of the sample (Fig. 3). In addition, $\sigma_r/\sigma_v$ is affected by $D/h$ for $\mu > 0$ (Fig. 3). Our results show that $\sigma_r/\sigma_v$, and hence $K_0$, is a function of $\nu$, $\mu$ and $D/h$. However, the impact of $\mu$ on overall sample behaviour can be minimised by using samples with large $D/h$ (Figs. 2 and 3).

### 4.3. Bulk density after compression

Changes in bulk density due to compression were found to be a function of $\sigma_{mean}$. $BD_{final}$ was uniform within the sample for $\mu$ = 0 (Figs. 2 and 5). In this case, and with the material properties used here (Tables 1 and 2) and $p_0$ = 200 kPa, $BD_{final}$ was 1.35 Mg m$^{-3}$ (Figs. 2, 5 and 6). However, for $\mu > 0$, $BD_{final}$ was not homogeneous within the sample, in accordance with the non-uniform stress field (Fig. 2). As seen for stress, $\mu$ had a larger relative impact on $BD_{final}$ for small $D/h$ (Fig. 5). For narrow samples (i.e. small $D/h$), a strong decrease in $BD_{final}$ with depth was observed, with $BD_{final}$ at the bottom of the sample only marginally larger than $BD_{initial}$ (*cf.* results shown in Fig. 2 for $D/h$ = 0.5). This explains findings by Schlüter and Vogel (2016) of a linear increase in porosity (corresponding to a decrease in BD) from the top to the bottom of their sample (12.5 mm diameter, ~26 mm height, corresponding to $D/h$ = 0.48) after compression.

The BD distribution within samples is typically not measured during uniaxial compression tests, which usually yield a sample-average BD value. We found (Fig. 6) that the sample-average BD after compression ($BD_{final,Mean}$) decreases (i.e. less compression) with increasing $\mu$, with the decrease being larger for small $D/h$ than for large $D/h$ (Fig. 6). Similarly, our experimental data show that the increase in BD due to compression increases with increasing $D/h$ (Fig. 7A). The impact of $\mu$ on $BD_{final,Mean}$ seems to be most pronounced for $\mu < 0.4$ (Fig. 6). Tuononen (2016) performed experiments with a rubber sample pressed against glass surfaces in a linear friction tester and found that an increase in $\mu$ did not change the contact conditions for $\mu > 0.5$ because the material fully adhered to the surface for $\mu > 0.5$.

The effects on $BD_{final,Mean}$ of $\mu$ and $D/h$ have consequences for the magnitude of compressive properties (e.g. compression index) obtained in uniaxial compression tests (strain, void ratio or bulk density as a function of the logarithm of applied stress). This is illustrated in Fig. 7B, which shows that the compression index is dependent on $D/h$. For the examples shown, the compression index ranged from 0.052 (samples with $D/h$ = 1) to 0.103 (samples with $D/h$ = 2.88) at 0.3 m depth and from 0.087 ($D/h$ = 1) to 0.116 ($D/h$ = 2.88) at 0.5 m depth, i.e. it decreased with increasing $D/h$ for both depths. Decreasing compression index with increasing sample height at constant sample diameter was also reported by Berli (2001). Hence, the compressibility of soil is underestimated for small $D/h$.

The effects of soil-cylinder wall friction on $BD_{final,Mean}$ can be significantly reduced by increasing $D/h$. However, Fig. 6 suggests that the impact of $\mu$ can only be neglected if $D/h$ is ~8 or larger. A $D/h$ value of 8 would not be practically feasible for collecting undisturbed samples of

arable soil in the field. Sample height cannot be smaller than a few centimetres in order to capture relevant soil structural features, for practical reasons (handling of samples in the field) and to minimise edge effects. Our results show that the error in $BD_{final,Mean}$ caused by neglecting soil-wall friction is of the order of magnitude of 1% for $D/h = 3$ (as suggested by Koolen, 1974) and 2% for $D/h = 1$. Small differences in BD can have significant effects on soil mechanical and hydraulic properties (Horn and Kutilek, 2009). A practical solution could be to correct $BD_{final,Mean}$ as a function of $\mu$ and $D/h$. This would allow e.g. direct comparison of data obtained in different laboratories that use different sample sizes.

## 5. Conclusions

We show that soil-cylinder wall friction significantly affects the distribution of stresses, and hence strains and bulk density pattern, within soil samples subjected to uniaxial compression. This has significant effects on sample-average bulk density and compressive properties (e.g. compression index, precompression stress) derived from this. The relative impact of soil-wall friction on sample-average behaviour decreases with increasing sample diameter to height ratio ($D/h$). These results obtained in simulations are supported by experimental data. Our simulation results suggest that the effect of soil-wall friction on sample-average bulk density cannot be neglected unless $D/h > 8$, but such large $D/h$ is not feasible for several reasons. We estimated that the error in bulk density caused by neglecting soil-wall friction is around 1% for $D/h = 3$ (often suggested as optimum $D/h$) and 2% for $D/h = 1$. Correction of bulk density as a function of the coefficient of soil-wall friction and $D/h$ is possible and would allow comparison of data obtained in laboratories using different sample sizes. Future research could establish 'correction factors' for comparing results across sample dimensions, which would allow data on compressive properties obtained in different laboratories to be used in developing pedo-transfer functions for soil compressive properties.

We show that the impact of soil-wall friction can be minimised by using a large $D/h$ or by correcting for soil-wall friction as a function of $D/h$. However, the stresses within the sample, and hence the ratio of radial to vertical stress and thus the mean normal stress, are a function of the soil Poisson's ratio. Because it cannot be measured in uniaxial compression tests, knowledge of the ratio of radial to vertical stress is essential to compute the mean normal stress, which in turn can be related to volumetric deformation (bulk density) to obtain compressive properties of soil. For large $D/h$, effects of soil-wall friction can be neglected and the ratio of radial to vertical stress becomes a function of the soil Poisson's ratio. We suggest that Poisson's ratio be measured and used in analysis of data and determination of compressive properties from uniaxial compression tests.

## Acknowledgements

The authors would like to thank the CAPES organisation of the Federal Government of Brazil for financial support that enabled the first author (Renato Paiva de Lima) to work for a period at Agroscope, Zürich, Switzerland. Thomas Keller would like to acknowledge financial support from the Swedish Farmers' Foundation for Agricultural Research (Stiftelsen Lantbruksforskning, SLF) through grant no. O-17-23-959.

## References

American Society for Testing and Material, 2010. D2435'. 'Standard Test Method for One-dimensional Consolidation Properties of Soils'.
Berli, M, 2001. Compaction of agricultural subsoils by tracked heavy construction machinery. Diss. ETH No. 14132.
British Standard, BS1377, 1990. Part 5. 'Methods of Tests for Soils for Civil Engineering Purposes - Compressibility, Permeability and Durability Tests'.
Davis, R.O., Selvadurai, A.P.S., 1996. Elasticity and Geomechanics. Cambridge University Press, Cambridge.
Défossez, P., Richard, G., Boizard, H., O'Sullivan, M.F., 2003. Modeling change in soil compaction due to agricultural traffic as function of soil water content. Geoderma 116, 89–105.
Eggers, C.G., Berli, M., Accorsi, M.L., Or, D., 2006. Deformation and permeability of aggregated soft earth materials. J. Geophys. Res. 111, B10204. https://doi.org/10.1029/2005JB004123.
Horn, R., Fleige, H., 2009. Risk assessment of subsoil compaction for arable soils in Northwest Germany at farm scale. Soil Till. Res. 102, 201–208.
Horn, R., Kutilek, M., 2009. The intensity-capacity concept – how far is it possible to predict intensity values with capacity parameters. Soil Till. Res. 103, 1–3.
Keller, T., Défossez, P., Weisskopf, P., Arvidsson, J., Richard, G., 2007. SoilFlex: a model for prediction of soil stresses and soil compaction due to agricultural field traffic including a synthesis of analytical approaches. Soil Till. Res. 93, 391–411.
Keller, T., Ruiz, S., Stettler, M., Berli, M., 2016. Determining soil stress beneath a tire: measurements and simulations. Soil Sci. Soc. Am. J. 80, 541–553.
Kirby, M.J., 1999. Soil stress measurement: part I. Transducer in a uniform stress field. J. Agric. Eng. Res. 72, 151–160.
Kolay, P., Bhattacharya, G., 2008. Remediation of the side friction in conventional oedometer tests by using large diameter consolidometer ring. Int. J. Geotech. Eng. 2, 161–167.
Koolen, 1974. A Method for soil compactibility determination. J. Agric. Eng. Res. 19, 271–278.
Koolen, A.J., Kuipers, H., 1983. Agricultural Soil Mechanics. Advanced Series in Agricultural Sciences, 13 241 Springer-Verlag, Berlin.
Lima, R.P., Silva, A.P., Giarola, N.F., Silva, A.R., Rolim, M.M., Keller, T., 2018. Impact of initial bulk density and matric suction on compressive properties of two Oxisols under no-till. Soil Till. Res. 175, 168–177.
McKenzie, B.M., Mullins, C.E., Tisdall, J., Bengough, G., 2013. Root-soil friction: quantification provides evidence for measurable benefits for manipulation of root-tip traits. Plant Cell Environ. 36, 1085–1092.
Musson, R.W., Carlson, W., 2014. Simulation of solitary waves in a monodisperse granular chain using COMSOL multiphysics: localized plastic deformation as a dissipation mechanism. Granul. Matter 16, 543–550.
Naderi-Boldaji, M., Alimardani, R., Hemmat, A., Sharifi, A., Keyhani, A., Tekeste, M.Z., Keller, T., 2014. 3D finite element simulation of a single-tip horizontal penetrometer-soil interaction. Part II: soil bin verification of the model in a clay-loam soil. Soil Till. Res. 144, 211–219.
Naderi-Boldaji, M., Hajian, A., Ghanbarian, D., Bahrami, M., 2018. Finite element simulation of plate sinkage, confined and semi-confined compression tests: A comparison of the response to yield stress. Soil Till. Res. 179, 63–70.
O'Sullivan, M.F., Robertson, E.A.G., 1996. Critical state parameters from intact sample of two agricultural soils. Soil Till. Res. 39, 161–173.
Rosine, T.N., Sabbagh, T.T., 2015. The impact of the diameter to height ratio on the compressibility parameters of saturated fine-grained soils. IJERT 4, 8–19.
Schjønning, P., van den Akker, J.J.H., Keller, T., Greve, M.H., Lamandé, M., Simojoki, A., Stettler, M., Arvidsson, J., Breuning-Madsen, H., 2015. Driver-Pressure-State-Impact-Response (DPSIR) analysis and risk assessment for soil compaction – a European perspective. Adv. Agron. 133, 183–237.
Schlüter, S., Vogel, H.J., 2016. Analysis of soil structure turnover with garnet particles and X-ray microtomography. Plos One 11, 1–17.
Stettler, M., Keller, T., Weisskopf, P., Lamandé, M., Lassen, P., Schjønning, P., 2014. Terranimo® – a web-based tool for evaluating soil compaction. Landtechnik 69, 132–137.
Taylor, D.W., 1942. Research on Consolidation of Clays. Massachusetts Institute of Technology, Cambridge, USA 147 pp.
Tsubakihara, Y., Kishida, H., Nishiyama, T., 1993. Friction between cohesive soils and steel. Soils Found 33, 145–156.
Tuononen, A.J., 2016. Onset of frictional sliding of rubber–glass contact under dry and lubricated conditions. Sci. Rep. 6, 27951.
van den Akker, J.J.H., Arvidsson, J., Horn, R., 2003. Introduction to the special issue on experiences with the impact and prevention of subsoil compaction in the European Union. Soil Till. Res. 73, 1–8.